

# CHEMISTRY

## A European Journal

A Journal of



### Accepted Article

**Title:** Aerobic Oxidation Catalysis by a Molecular Barium Vanadium Oxide

**Authors:** Manuel Lechner, Katharina Kastner, Chee Jian Chan, Robert Güttel, and Carsten Streb

This manuscript has been accepted after peer review and appears as an Accepted Article online prior to editing, proofing, and formal publication of the final Version of Record (VoR). This work is currently citable by using the Digital Object Identifier (DOI) given below. The VoR will be published online in Early View as soon as possible and may be different to this Accepted Article as a result of editing. Readers should obtain the VoR from the journal website shown below when it is published to ensure accuracy of information. The authors are responsible for the content of this Accepted Article.

**To be cited as:** *Chem. Eur. J.* 10.1002/chem.201706046

**Link to VoR:** <http://dx.doi.org/10.1002/chem.201706046>

Supported by  
**ACES**

WILEY-VCH

## COMMUNICATION

## Aerobic Oxidation Catalysis by a Molecular Barium Vanadium Oxide

Manuel Lechner,<sup>[a]</sup> Katharina Kastner,<sup>[a]</sup> Chee Jian Chan,<sup>[c]</sup> Robert Güttel<sup>[c]\*</sup> and Carsten Streb<sup>[a,b]\*</sup>Dedicated to Professor Achim Müller (Bielefeld) on the occasion of his 80<sup>th</sup> birthday

**Abstract:** Aerobic catalytic oxidations are promising routes to replace environmentally harmful oxidants with O<sub>2</sub> in organic syntheses. Here, we report a molecular barium vanadium oxide, [Ba<sub>4</sub>(dmsO)<sub>14</sub>V<sub>14</sub>O<sub>38</sub>(NO<sub>3</sub>)] (= {Ba<sub>4</sub>V<sub>14</sub>}) as viable homogeneous catalyst for a series of oxidation reactions in N,N-dimethyl formamide solution under oxygen (8 bar). Starting from the model compound 9,10-dihydroanthracene, we report initial dehydrogenation / aromatization leading to anthracene formation; this intermediate is subsequently oxidized by stepwise oxygen transfer, first giving the mono-oxygenated anthrone and then the di-oxygenated target product, anthraquinone. Comparative reaction analyses using the Neumann catalyst [PV<sub>2</sub>Mo<sub>10</sub>O<sub>40</sub>]<sup>5-</sup> as reference show that oxygen diffusion into the reaction mixture is the rate-limiting step, resulting in accumulation of the reduced catalyst species. This allows us to propose improved reactor designs to overcome this fundamental challenge for aerobic oxidation catalysis.

## Introduction

The selective catalytic oxidation of organic substrates is one of the most important reaction classes in chemistry as it gives access to a wide range of (partially) oxidized compounds ranging from bulk to fine chemicals.<sup>[1,2]</sup> Often, solid-state metal oxides (e.g. V<sub>2</sub>O<sub>5</sub>) are used as catalysts due to their high activity and long-term stability. However, over the last decade, liquid phase operations have led to a renewed interest in soluble molecular metal oxides, so-called polyoxometalates (POMs) as homogenous oxidation catalysts, particularly when low-temperature aerobic oxidations (using molecular O<sub>2</sub> as oxidant) are targeted.<sup>[3]</sup> POMs are polynuclear metal oxide anions typically based on early transition metals in their highest oxidation states (e.g. Mo<sup>VI</sup>, W<sup>VI</sup>, V<sup>V</sup>), see Fig. 1.

The presence of several redox-active metal centers together with oxo ligands on the cluster surface makes POMs ideally suited for proton-coupled multi-electron transfer reactions.<sup>[3,4]</sup> Their high activity, stability and catalytic selectivity together with the use of environmental friendly O<sub>2</sub> as re-oxidant have led to an increased interest in POM catalysts for the conversion of base

petrochemicals (alkanes, aromatics)<sup>[5]</sup> and biogenic feedstocks<sup>[6–8]</sup> to value-added products. Their versatility is illustrated by a variety of catalytic oxidations most notably C-H-activations,<sup>[9]</sup> epoxidations,<sup>[10]</sup> hydroxylations and more recently, water oxidation.<sup>[11,12]</sup>

To-date, aerobic POM oxidation catalysis is mainly focused on Keggin-type vanadomolybdate clusters of the type [PV<sub>x</sub>Mo<sub>12-x</sub>O<sub>40</sub>] (x = 2, 3, 4) with a particular focus on the heteropolyacid H<sub>5</sub>[PV<sub>2</sub>Mo<sub>10</sub>O<sub>40</sub>] = {V<sub>2</sub>Mo<sub>10</sub>}. Using this compound,<sup>[13]</sup> Neumann *et al.* have performed pioneering catalytic and mechanistic studies and reported catalytic activity for C-H activation,<sup>[14]</sup> aromatic oxidation,<sup>[15]</sup> epoxidation,<sup>[16]</sup> oxidative dimerization and aromatization<sup>[17]</sup> reactions.<sup>[13]</sup> Notably, the authors proposed that the oxidative catalytic activity is based on a Mars-van-Krevelen mechanism<sup>[14,18]</sup> where the oxygen atom transferred to the substrate originates from the cluster oxo ligands, not from molecular oxygen.<sup>[13]</sup> This is a critical observation, as it could enable the de-coupling of substrate oxidation and catalyst re-oxidation, thereby eliminating uncontrolled O<sub>2</sub>-based autoxidation reactions.<sup>[19]</sup> In a recent landmark paper, Neumann *et al.* demonstrated that {V<sub>2</sub>Mo<sub>10</sub>} can be used for the liquid phase chemical/electrochemical conversion of cellulose or hemicellulose to carbon monoxide and hydrogen, i.e. syngas, showing the potential use of the catalyst in the field of non-fossil chemical feedstocks.<sup>[20]</sup> Related studies by Albert, Wasserscheid *et al.* have led to the industrial OxFA process where {V<sub>2</sub>Mo<sub>10</sub>} is used as catalyst for the aerobic oxidative conversion of wet biomass to formic acid.<sup>[6–8]</sup>

These seminal works show that POM-catalyzed aerobic oxidations are critical reactions for the sustainable chemical oxidations with industrial relevance. However, the use of O<sub>2</sub> as benign oxidant<sup>[21]</sup> results in new challenges, as the biphasic reaction systems require not only the development of high performance catalysts, but at the same time, novel reactor design paradigms are required to prevent mass transfer limitations due to the slow diffusion of O<sub>2</sub> into the liquid reaction mixtures.<sup>[22]</sup>

We have recently started to investigate metal-functionalized polyoxovanadates<sup>[23–25]</sup> as potential catalysts for chemical or photochemical oxidations.<sup>[26–31]</sup> To enable a targeted metal-functionalization of vanadate clusters, we developed a chloride-templated vanadate “host” cluster (Me<sub>2</sub>NH<sub>2</sub>)<sub>2</sub>[V<sub>12</sub>O<sub>32</sub>Cl]<sup>3-</sup> (= {V<sub>12</sub>}) featuring two Me<sub>2</sub>NH<sub>2</sub><sup>+</sup>-blocked metal binding sites.<sup>[26,27,32–34]</sup> Incorporation of one or two reactive 3d metal “guests” is possible, leading to metal-functionalized vanadates as multi-electron transfer sites,<sup>[27,32]</sup> e.g. in battery electrodes<sup>[34]</sup> or as catalysts for C-H-activation<sup>[27]</sup> and alcohol oxidation.<sup>[33]</sup> Based on these studies, we became interested in expanding this “host-guest” assembly strategy by developing a vanadate “host” capable of binding larger metals, e.g. large alkali or alkali earth cations. A specific focus was set on the incorporation of barium centers, as solid-state

[a] M. Sc. M. Lechner, Dr. K. Kastner, Prof. Dr. C. Streb  
Institute of Inorganic Chemistry I  
Ulm University  
Albert-Einstein-Allee 11, 89081 Ulm (Germany)  
E-mail: carsten.streb@uni-ulm.de

[b] Prof. Dr. C. Streb  
Helmholtz Institute Ulm for Electrochemical Energy Storage, 89081  
Ulm, Germany and Karlsruhe Institute of Technology, P.O. Box  
3640, 76021 Karlsruhe, Germany

[c] PgDipSc. A. Chan, Prof. Dr.-Ing. R. Güttel  
Institute of Chemical Engineering  
Ulm University  
Albert-Einstein-Allee 11, 89081 Ulm (Germany)  
Email: robert.guettel@uni-ulm.de

## COMMUNICATION

barium vanadates are well-known oxidation catalysts, e.g. for alkane dehydrogenation<sup>[35]</sup> or selective methanol oxidation.<sup>[36]</sup> Here, we report the synthesis of a novel vanadate “host” featuring an enlarged binding site suitable for binding four Ba<sup>2+</sup> centers. Enlargement of the binding site was possible by using nitrate as an internal template, while in {V<sub>12</sub>}, a smaller chloride template was used. The new cluster is fully characterized in the solid-state and in solution. Initial aerobic oxidation studies show the high reactivity of the catalyst and emphasize that future aerobic catalytic studies need to focus on optimizing the oxygen transfer into the liquid phase to improve catalytic efficiency.

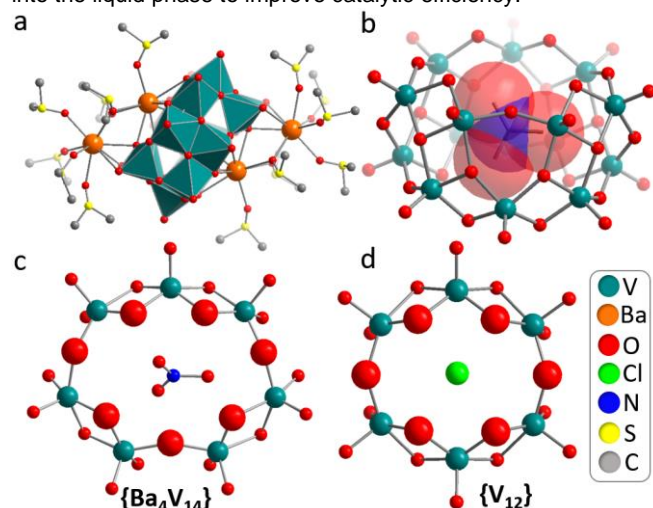


**Figure 1:** (a) structural representation of {Ba<sub>4</sub>V<sub>14</sub>}, Ba<sub>4</sub>(dmsO)<sub>14</sub>[V<sub>14</sub>O<sub>38</sub>(NO<sub>3</sub>)]. (b) {V<sub>14</sub>} cluster framework showing the template NO<sub>3</sub><sup>-</sup>. (c), (d) Comparison of the metal binding sites in the literature-known, chloride-templated {V<sub>12</sub>}<sup>[26,27]</sup> and the nitrate-templated {Ba<sub>4</sub>V<sub>14</sub>}. Colour scheme: Ba: orange, V: teal, O: red, Cl: green, N: blue, S: yellow, C: grey.

## Results

Synthesis and characterization of {Ba<sub>4</sub>V<sub>14</sub>}

(*n*Bu<sub>4</sub>N)<sub>4</sub>[V<sub>4</sub>O<sub>12</sub>] • 4 H<sub>2</sub>O (= {V<sub>4</sub>}) and Ba(NO<sub>3</sub>)<sub>2</sub> were reacted in dimethyl sulfoxide (DMSO) in the presence of aqueous nitric acid. Diffusion of acetone into the deep red solution gave red block crystals suitable for single-crystal X-ray diffraction (yield: 7.13 g, 2.35 mmol, 98% based on V). Single-crystal X-ray diffraction gave the formula [Ba<sub>4</sub>(dmsO)<sub>14</sub>V<sub>14</sub>O<sub>38</sub>(NO<sub>3</sub>)] (= {Ba<sub>4</sub>V<sub>14</sub>}), see Fig. 1. Chemical composition and bulk purity were verified by elemental analyses, FT-IR-, UV-Vis spectroscopies and ESI mass spectrometry and cyclic voltammetry, see SI. {Ba<sub>4</sub>V<sub>14</sub>} is composed of 14 square pyramidal [VO<sub>5</sub>] units arranged around a central nitrate template, giving a C<sub>2v</sub>-symmetric vanadium oxide shell. Long-range electrostatic interactions between the nitrate oxygen atoms and the V centers are indicated by the corresponding V...O separations (*d*(V...O(NO<sub>3</sub><sup>-</sup>)) ~2.90 – 3.14 Å). Notably, the belt-shaped vanadium oxide arrangement results in the formation of two binding sites on top and bottom of the cluster shell where formally, seven bridging oxo ligands form a heptadentate binding site with approximate dimensions of 0.7 x 0.5 nm (Fig. 1).

In {Ba<sub>4</sub>V<sub>14</sub>}, one Ba<sup>2+</sup> ion is bound at each binding site through five Ba-O coordination bonds (*d*(Ba-O) = 2.82 – 3.02 Å). In addition, a second Ba<sup>2+</sup> center is linked to the vanadium oxide through one Ba-O coordination bond (*d*(Ba-O) = 2.78 Å). The two

barium centers are bridged by two μ<sub>2</sub>-DMSO ligands and feature five additional, terminal DMSO ligands for stabilization. Each Ba center therefore is nine-coordinate in a distorted coordination polyhedron, see SI. All V-O and Ba-O distances are in line with the expected values reported in the literature.<sup>[37,38]</sup> Initial electrochemical studies by cyclic voltammetry (in N,N-dimethyl formamide containing 0.1 M *n*Bu<sub>4</sub>NPF<sub>6</sub>) show that {Ba<sub>4</sub>V<sub>14</sub>} features one reversible redox-wave at *E*<sub>1/2</sub> = 0.64 V (vs Fc/Fc<sup>+</sup>), see SI.

## Aerobic catalytic studies

To assess the general utility of {Ba<sub>4</sub>V<sub>14</sub>} as homogeneous aerobic (i.e. O<sub>2</sub>-dependent) oxidation catalyst, we examined the well-understood aerobic oxidation of 9,10-dihydroanthracene (DHA) to anthraquinone as a model reaction (Fig. 2). This reaction was pioneered by Neumann *et al.* using {V<sub>2</sub>Mo<sub>10</sub>} as homogeneous catalyst.<sup>[13]</sup> To compare the performance of {Ba<sub>4</sub>V<sub>14</sub>}, we therefore used the Neumann-catalyst {V<sub>2</sub>Mo<sub>10</sub>} as reference. For {V<sub>2</sub>Mo<sub>10</sub>}, it was shown that the oxidation is a three-step process where oxidative dehydrogenation of DHA to anthracene is followed by two oxygenation steps to give anthraquinone (Fig. 2).<sup>[22]</sup>

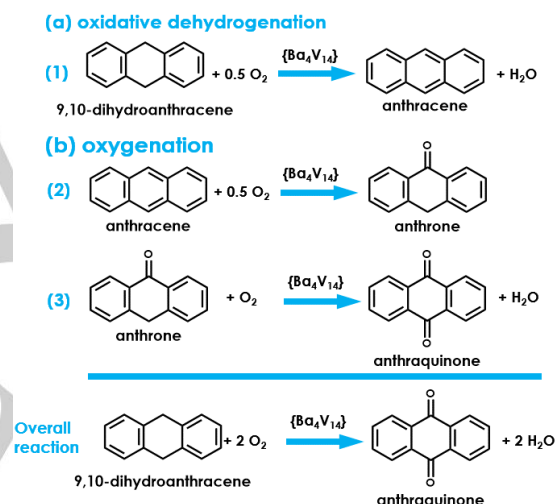


**Figure 2:** Reaction scheme for the two-step oxidation of DHA to anthraquinone catalyzed by {Ba<sub>4</sub>V<sub>14</sub>}.

The catalytic test reaction was carried out in N,N-dimethyl formamide (DMF) at *T* = 80 °C and *p*(O<sub>2</sub>) = 4–8 bar in a 50 mL discontinuous magnetically stirred glass pressure reactor. The initial concentration of the substrate DHA was 46 mM and the respective catalyst concentration was 0.9 mM (2 mol-% with respect to DHA). The formation of the intermediates anthracene, anthrone and the product anthraquinone was quantified using high-pressure liquid chromatography (HPLC). Note that the initial “induction phase” observed between *t* = 0–1 h (Fig. 3) is most likely due to the heating up of the reactor, as the starting point of the reaction (*t* = 0 h) was defined as switch-on of the reactor heating. This was experimentally the most consistent approach for full data collection.

As shown in Figure 3, catalytic conversion of DHA to anthracene, anthrone and anthraquinone is observed for {Ba<sub>4</sub>V<sub>14</sub>} and {V<sub>2</sub>Mo<sub>10</sub>}. Under identical conditions, the rates of anthraquinone formation are comparable for both catalysts. However, an earlier onset of anthraquinone formation is observed for {Ba<sub>4</sub>V<sub>14</sub>} so that at the defined end of the reaction (*t* = 7 h), higher yields of

## COMMUNICATION

anthraquinone are observed for  $\{\text{Ba}_4\text{V}_{14}\}$  (40 %) compared with  $\{\text{V}_2\text{Mo}_{10}\}$  (28 %). To understand this diverging behavior, we investigated the formation of the reaction intermediates anthracene and anthrone by both catalysts (Fig. 3). It was noted that for  $\{\text{Ba}_4\text{V}_{14}\}$ , very little accumulation of the intermediate anthracene (less than 2 % over the whole course of the reaction) is observed while significant amounts of anthrone are formed (up to ~15 % at  $t = 3$  h). For  $\{\text{V}_2\text{Mo}_{10}\}$ , we note a higher amount of anthracene accumulation (maximum ~8 % at  $t = 3$  h) while anthrone accumulation is only noted in later reaction phases (maximum ~11 % at  $t = 7$  h). This suggests that for  $\{\text{Ba}_4\text{V}_{14}\}$ , the anthracene to anthraquinone reaction steps proceed faster than for  $\{\text{V}_2\text{Mo}_{10}\}$ . These findings also explain the observed difference in anthraquinone yield after  $t = 7$  h: while for  $\{\text{Ba}_4\text{V}_{14}\}$ , we observe a fast conversion of anthracene to the oxidized products,  $\{\text{V}_2\text{Mo}_{10}\}$  leads to an accumulation of anthracene, which results in a later onset of anthraquinone formation. Based on literature reports<sup>[13]</sup> as well as the structural similarities between  $\{\text{V}_2\text{Mo}_{10}\}$  and  $\{\text{Ba}_4\text{V}_{14}\}$  and the known redox-activity of vanadium, we suggest that the V centres are the catalytically active sites, while the role of the Ba centres is currently not fully understood.

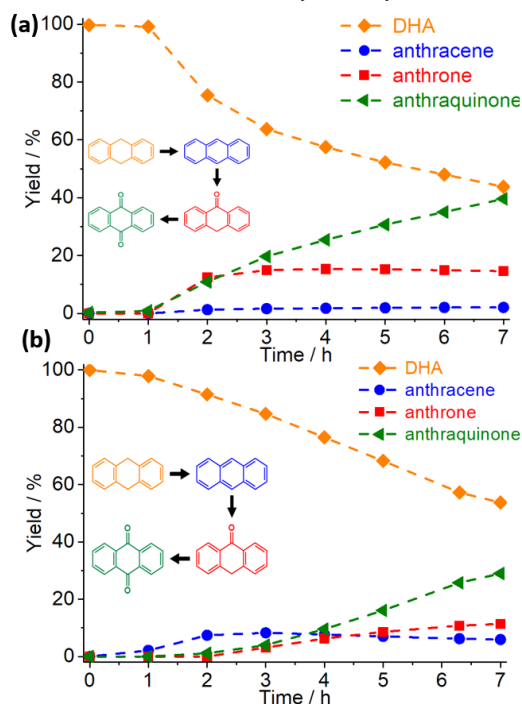


**Figure 3:** Aerobic oxidation of DHA using (a)  $\{\text{Ba}_4\text{V}_{14}\}$  and (b)  $\{\text{V}_2\text{Mo}_{10}\}$  as catalyst. Conditions:  $p(\text{O}_2) = 8$  bar,  $T = 80$  °C, solvent: DMF,  $[\text{cat}] = 0.9$  mM,  $[\text{DHA}] = 46$  mM.

The similar rates of anthraquinone formation observed for both catalysts led us to suggest that the reaction is mass transfer limited due to the slow diffusion of  $\text{O}_2$  from the gas phase into the liquid reaction mixture.<sup>[22]</sup> To verify this hypothesis, we performed the catalytic reaction at varying concentrations of the catalyst ( $[\{\text{Ba}_4\text{V}_{14}\}] = 0.45 - 1.8$  mM). The results show that within experimental error ( $\pm 3$  %) the rate of anthraquinone formation is independent of the catalyst concentration in the concentration range investigated (0.45 mM: 8.9 %/h; 0.9 mM: 9.5 %/h; 1.8 mM: 7.1 %/h), see Fig. 4 and SI. *In situ* UV-vis spectrometry of the reaction solution indicated that with progressing reaction time,

reduced  $\{\text{Ba}_4\text{V}_{14}\}$  is accumulated (as identified by the formation of a characteristic intervalence charge-transfer band at  $\lambda \sim 600$ –900 nm, see SI). This supports the suggestion that catalyst re-oxidation by dissolved  $\text{O}_2$  is limiting the overall reaction. In sum, our findings are in line with previous studies by Neumann *et al.* who observed that re-oxidation of  $\{\text{V}_2\text{Mo}_{10}\}$  is rate-limiting for the anthracene-to-anthraquinone oxidation.<sup>[17]</sup>

Next, we assessed whether  $\{\text{Ba}_4\text{V}_{14}\}$  can be recovered from solution and can be recycled. To this end, the catalyst was precipitated from the reaction solution by addition of diethyl ether, centrifuged off, air-dried and re-dissolved in a fresh reaction mixture to perform our standard aerobic DHA oxidation. The results showed that recycling is possible and only minor changes in the initial product formation rates was observed (run 1: 8.9 %/h; run 2: 11.2 %/h; run 3: 7.8 %/h, see SI). UV-Vis spectroscopy of the recycled catalyst shows similar characteristic absorption features than the native catalyst, see SI. Intriguingly, we noted an increase of the “induction period” described earlier. This might be related to an initial re-oxidation step required for catalyst activation and is still under investigation. Further mechanistic studies will explore the detailed changes of  $\{\text{Ba}_4\text{V}_{14}\}$  structure and reactivity during recycling.

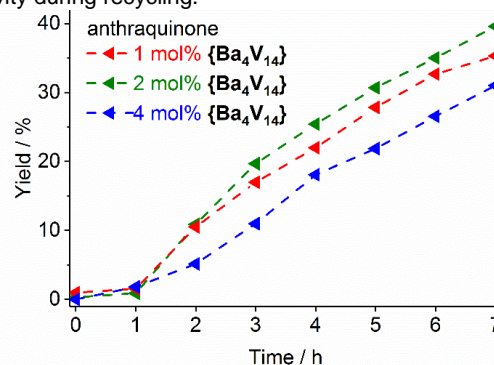


**Figure 4:** Similar anthraquinone formation rates observed for the catalytic aerobic oxidation of DHA at different  $\{\text{Ba}_4\text{V}_{14}\}$  concentrations, indicating that catalytic turnover is not rate-limiting. Conditions:  $p(\text{O}_2) = 8$  bar,  $T = 80$  °C, solvent: DMF,  $[\text{cat}] = 0.45$  mM (1 mol%), 0.9 mM (2 mol%), 1.8 mM (4 mol%),  $[\text{DHA}] = 46$  mM.

**Table 1:** Catalytic DHA conversion by POM catalysts<sup>[a]</sup>

Catalyst	[Cat] / mM	Reaction time / h	DHA conversion / %	Initial anthraquinone formation rate / %h <sup>-1</sup>
$\{\text{Ba}_4\text{V}_{14}\}$	0.90	7	59.5	9.5
$\{\text{Ba}_4\text{V}_{14}\}$	0.90	16	71.3	-
$\{\text{V}_2\text{Mo}_{10}\}$	0.90	7	46.3	7.4
$\{\text{V}_2\text{Mo}_{10}\}$	0.90	16	71.5	-
$\{\text{V}_4\}$	3.16 <sup>[b]</sup>	7	9.4	1.9
$\{\text{V}_4\} + \text{Ba}(\text{NO}_3)_2$	3.16 <sup>[b]</sup>	7	15.7	3.3
$(n\text{Bu}_4\text{N})_3[\text{H}_3\text{V}_{10}\text{O}_{28}]$	1.27 <sup>[b]</sup>	7	31.4	3.2

<sup>[a]</sup> conditions: solvent: DMF,  $p = 8$  bar  $\text{O}_2$ ,  $T = 80$  °C; <sup>[b]</sup> the cluster concentration was chosen to give identical vanadium concentrations in solution as for  $\{\text{Ba}_4\text{V}_{14}\}$  (i.e.  $14 \times 0.9$  mM = 12.6 mM).



## COMMUNICATION

Finally, we compared the catalytic performance of  $\{\text{Ba}_4\text{V}_{14}\}$  and  $\{\text{V}_2\text{Mo}_{10}\}$  with the iso-polyoxovanadates  $\{\text{V}_4\}$ ,  $[\text{H}_3\text{V}_{10}\text{O}_{28}]^{3-}$  and a mixture of  $\{\text{V}_4\}$  and  $\text{Ba}^{2+}$  (i.e. the components used to form  $\{\text{Ba}_4\text{V}_{14}\}$ ) to establish the importance of the cluster structure and to verify that the presence of a vanadate moiety is not sufficient for effective DHA oxidation catalysis. As shown in Table 1, under identical experimental conditions (and identical vanadium concentrations), we note significantly higher rates of anthraquinone formation for  $\{\text{Ba}_4\text{V}_{14}\}$  and  $\{\text{V}_2\text{Mo}_{10}\}$  compared with the reference components. While this initial result does not provide deep mechanistic insight into the role of the cluster structure, it nevertheless emphasizes that structural control and modification of molecular vanadium oxides is a viable tool to optimize the oxidative catalytic reactivity.

In sum, this study demonstrates that the development of new aerobic oxidation catalysts needs to be combined with advanced reactor design considerations to achieve maximum catalytic performance. Examples of suitable reactor types to maximize  $\text{O}_2$  transfer into the liquid phase for the system presented are currently under investigation and could involve e.g. bubble column or biphasic microflow reactors.<sup>[22]</sup>

## Experimental Section

**Synthesis of  $\{\text{Ba}_4\text{V}_{14}\}$ :**  $(n\text{Bu}_4\text{N})_4[\text{V}_4\text{O}_{12}] \cdot 4 \text{H}_2\text{O}$  ( $= \{\text{V}_4\}$ ; 12 g, 8.35 mmol, 1 eq.) was reacted with  $\text{Ba}(\text{NO}_3)_2$  (5.8 g, 22.2 mmol, 2.66 eq.) in dimethyl sulfoxide (DMSO, 180 ml). The solution was stirred at 70°C for 4 h. After cooling the yellow solution to room temperature, aqueous nitric acid (3 M, 6.25 mL) was added dropwise and the solution turned deep red. The solution was stirred for 2 h at room temperature. Diffusion of acetone or ethyl acetate into the mother liquor gave red block crystals suitable for single-crystal X-ray diffraction. The red crystals were filtered off, washed with acetone and diethyl ether and were air-dried. Yield: 7.13 g, 2.35 mmol, 98 % based on V. Elemental analysis of  $\text{C}_{28}\text{H}_{84}\text{Ba}_4\text{NO}_{55}\text{S}_{14}\text{V}_{14}$  (calculated values in brackets): C 11.09 (C 11.11), H 2.89 (H 2.80), N 0.60 (N 0.46), S 14.68 (S 14.83), Ba 17.34 (Ba 18.15), V 20.44 (V 23.57). FT-IR spectroscopy (in  $\text{cm}^{-1}$ ): 2998 (w), 2912 (w), 1434 (w), 1386 (m), 1314 (w), 1026 (vs), 988 (vs), 957 (m), 854 (m), 822 (m), 758 (m), 703 (m), 629 (s).

**Catalytic test reaction:** The oxidation experiments were performed in a *miniclave steel* laboratory pressure reactor system from *büchiglas* using a normal stir bar for mixing. Therefore 46 mM of substrate (DHA) where dissolved together with 0.45 – 1.8 mM of catalyst in 50 mL DMF and put into the pressure reactor. The pressure of pure oxygen (4 – 8 bar) could be varied and monitored with a pressure gauge. With the integrated sample taking system it was possible to take a sample out of the reactor every hour. An exact volume of 0.5 mL of reaction mixture was taken out and added to 4 mL of diethyl ether to precipitate the catalyst. After centrifuging the mixture, the reaction products could easily be separated from the catalyst and 1.5 mL of this clear solution were transferred into HPLC-vials and stored in the fridge. To quantify the reaction components (DHA, anthracene, anthrone, anthraquinone) a HPLC system was used.

**High performance liquid chromatography (HPLC):** HPLC was used to quantify the reaction components. Therefore, a PerkinElmer Altus A-10 solvent and sample module with a separation module and a column oven was used. For detection an Altus A-10 PDA detector was used together with a C18 symmetry column (Waters). The following solvent mixtures were used for product elution: phase 1: linear gradient (for 20 min elution time) from MeCN:H<sub>2</sub>O (4:6) to MeCN:H<sub>2</sub>O (7:3); phase 2: further elution for 15 min at MeCN:H<sub>2</sub>O (7:3). Calibration curves of pure DHA, anthracene, anthrone and anthraquinone were used to calculate the reagent conversion and intermediate/product yield.

## Acknowledgements

The Vector Foundation and Ulm University are gratefully acknowledged for financial support.

**Keywords:** Polyoxometalate • Polyoxovanadate • Catalysis • Self-Assembly • Oxidation

## Notes and references

- [1] C. D. Weber, C. Bradley, M. C. Lonergan, *J. Mater. Chem.* **2014**, 2, 303.
- [2] J. S. J. Hargreaves, D. S. Jackson, *Metal Oxide Catalysis*, WILEY-VCH Verlag Weinheim, **2009**.
- [3] S. Wang, G. Yang, *Chem. Rev.* **2015**, 115, 4893–4962.
- [4] C. L. Hill, *J. Mol. Catal. A Chem.* **2007**, 262, 2–6.
- [5] C. L. Hill, C. M. Prosser-McCarthy, *Coord. Chem. Rev.* **1995**, 143, 407–455.
- [6] J. Reichert, B. Brunner, A. Jess, P. Wasserscheid, J. Albert, *Energy Environ. Sci.* **2015**, 8, 2985–2990.
- [7] J. Albert, R. Wölfel, A. Bösmann, P. Wasserscheid, *Energy Environ. Sci.* **2012**, 5, 7956.
- [8] J. Albert, P. Wasserscheid, *Green Chem.* **2015**, 17, 5164–5171.
- [9] K. Kamata, K. Yonehara, Y. Nakagawa, K. Uehara, N. Mizuno, *Nat Chem* **2010**, 2, 478–483.
- [10] N. Mizuno, K. Yamaguchi, K. Kamata, *Coord. Chem. Rev.* **2005**, 249, 1944–1956.
- [11] A. Sartorel, M. Carraro, F. M. Toma, M. Prato, M. Bonchio, *Energy Environ. Sci.* **2012**, 5, 5592.
- [12] H. Lv, Y. V. Geletii, C. Zhao, J. W. Vickers, G. Zhu, Z. Luo, J. Song, T. Lian, D. G. Musaev, C. L. Hill, *Chem. Soc. Rev.* **2012**, 41, 7572.
- [13] R. Neumann, *Inorg. Chem.* **2010**, 49, 3594–3601.
- [14] A. M. Khenkin, L. Weiner, Y. Wang, R. Neumann, *J. Am. Chem. Soc.* **2001**, 123, 8531–8542.
- [15] A. M. Khenkin, R. Neumann, C. M. Che, Z. Mao, V. M. Miskowski, M. C. Tse, C. K. Chan, K. K. Cheung, D. L. Phillips, K. H. Leung, A. M. Khenkin, R. Neumann, *Angew. Chemie* **2000**, 39, 4088–4090.
- [16] W. Adam, P. L. Alsters, R. Neumann, C. R. Saha-Möller, D. Sloboda-Rozner, R. Zhang, *J. Org. Chem.* **2003**, 68, 1721–1728.
- [17] R. Neumann, M. Levin, *J. Am. Chem. Soc.* **1992**, 114, 7278–7286.
- [18] C. Doornkamp, V. Ponec, *J. Mol. Catal. A Chem.* **2000**, 162, 19–32.
- [19] T. Punniyamurthy, S. Velusamy, J. Iqbal, *Chem. Rev.* **2005**, 105, 2329–2364.
- [20] B. B. Sarma, R. Neumann, *Nat. Commun.* **2014**, 5, 4621.
- [21] G.-J. ten Brink, I. W. C. E. Arends, R. A. Sheldon, *Science* **2000**, 287, 1636–1639.
- [22] M. Lechner, R. Güttel, C. Streb, *Dalton Trans.* **2016**, 45, 16716–16726.
- [23] C. Streb, Springer Verlag, Berlin, Heidelberg, **2017**, pp. 1–17.
- [24] W. G. Klempner, T. A. Marquart, O. M. Yaghi, *Angew. Chem. Int. Ed. Engl.* **1992**, 31, 49–51.
- [25] Y. Hayashi, *Coord. Chem. Rev.* **2011**, DOI: 10.10.
- [26] K. Kastner, J. T. Margraf, T. Clark, C. Streb, *Chem. Eur. J.* **2014**, 20, 12269–12273.
- [27] K. Kastner, J. Forster, H. Ida, G. N. G. N. Newton, H. Oshio, C. Streb, *Chem. Eur. J.* **2015**, 21, 7686–7689.

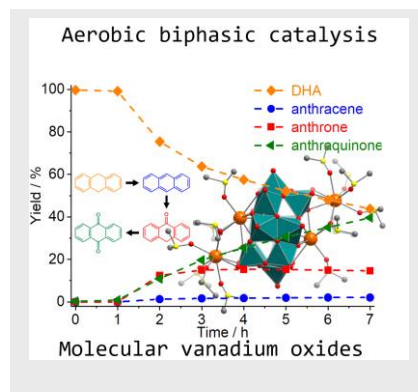
## COMMUNICATION

- [28] J. Tucher, C. Streb, *Beilstein J. Nanotechnol.* **2014**, *5*, 711–716.
- [29] J. Tucher, L. C. L. C. Nye, I. Ivanovic-Burmazovic, A. Notarnicola, C. Streb, *Chem. Eur. J.* **2012**, *18*, 10949–10953.
- [30] A. Seliverstov, C. Streb, *Chem. Eur. J.* **2014**, *20*, 9733–9738.
- [31] B. Schwarz, J. Forster, M. K. Goetz, D. Yücel, C. Berger, T. Jacob, C. Streb, *Angew. Chem. Int. Ed.* **2016**, *55*, 6329–6333.
- [32] M. H. Anjass, K. Kastner, F. Nägele, M. Ringenberg, J. F. Boas, J. Zhang, A. M. Bond, T. Jacob, C. Streb, *Angew. Chem. Int. Ed.* **2017**, *56*, 14749–14752.
- [33] K. Kastner, M. Lechner, S. Weber, C. Streb, *ChemistrySelect* **2017**, *2*, 5542–5544.
- [34] Y. Ji, J. Hu, J. Biskupek, U. Kaiser, Y.-F. Song, C. Streb, *Chem. Eur. J.* **2017**, *23*, 16637–16643.
- [35] E. A. Mamedov, V. Cortés Corberán, *Appl. Catal. A, Gen.* **1995**, *127*, 1–40.
- [36] I. Wachs, L. Briand, US Patent No US20050038299, **2005**
- [37] K. Kastner, B. Puscher, C. Streb, *Chem. Commun.* **2013**, *49*, 140–142.
- [38] K. Kastner, C. Streb, *CrystEngComm* **2013**, *15*, 4948.

## COMMUNICATION

## FULL PAPER

The first molecular barium vanadium oxide catalyst is reported. The compound,  $[\text{Ba}_4(\text{dmsO})_{14}\text{V}_{14}\text{O}_{38}(\text{NO}_3)]$ , is capable of the three-step aerobic oxidation of the model reagent 9,10-dihydroanthracene to anthraquinone, it can be recycled without loss of activity and provides critical insights into the challenges arising from liquid-gas phase catalysis using  $\text{O}_2$  as environmentally benign oxidant.



M. Lechner, K. Kastner, C.J. Chan, R. Güttel, \* C. Streb\*

Page No. – Page No.

Aerobic Oxidation Catalysis by a Molecular Barium Vanadium Oxide